SANDIA REPORT SAND82—1043 • Unlimited Release • UC—70
Printed August 1984

Water Transport Through Welded Tuff

G. Ronald Hadley

Prepared by
Sandia National Laboratories
Albuquerque, New Mexico 87185 and Livermore, California 94550
for the United States Department of Energy
under Contract DE-AC04-76DP00789

Issued by Sandia National Laboratories, operated for the United States Department of Energy by Sandia Corporation.

Printed in the United States of America
Available from
National Technical Information Service
U.S. Department of Commerce
5285 Port Royal Road
Springfield, VA 22161

NTIS price codes
Printed copy: A03
Microfiche copy: A01

SAND82-1043
Printed August 1984
Unlimited Release

Distribution
UC-70

WATER TRANSPORT THROUGH WELDED TUFF*

G. Ronald Hadley
Fluid Mechanics and Heat Transfer Division I
Sandia National Laboratories
Albuquerque, New Mexico 87185

ABSTRACT

Water transport through welded tuff was studied with the aid of three drying experiments and one imbibition experiment performed on a single 0.15 m long core. The specimen was saturated using a novel technique which measures the volume of water imbibed as a function of time in order to insure complete saturation. Profiles of saturation vs. axial position along the core were provided by measuring the intensity of a beam of 662 keV gamma ray photons after passing through the sample in a direction normal to the axis of the cylinder. Measurements were made at different axial locations by moving the sample chamber past the beam with a precision translation table. Results indicate that the drying process is, in general, not characterized by a receding evaporation front as has been previously assumed, but rather by evaporation throughout the sample. Water appears to move through the sample under the action of both capillary forces and vapor pressure gradients induced by temperature gradients. Profiles resembling those of a receding evaporation front were observed when the temperature gradient was aligned in the direction of moisture transport. This work was performed in support of the Nevada Nuclear Waste Storage Investigation Project, which is responsible for examining the feasibility of siting a repository for commercial high level nuclear wastes at Yucca Mountain and adjacent to the Nevada Test Site.

*This work performed at Sandia National Laboratories supported by the U.S. Department of Energy under Contract No. DE-AC04-76DP00789.

CONTENTS

NOMENCLATURE

English Symbols

I	beam intensity (photons/s)
ℓ	beam path length
N	number of counts
R	count rate (photons/s)
s	saturation (fraction of total void volume filled with water)
t	count time (s)
z	material thickness

Greek Symbols

γ	atomic absorption coefficient (m^2/kg)
ϕ	porosity
ρ	material density
τ	electronics response time (s)

Subscripts

wet	100% saturation
dry	0% saturation

LIST OF FIGURES

I. INTRODUCTION

The Nevada Nuclear Waste Storage Investigations Project, managed by the Nevada Operations Office of the U.S. Department of Energy, is examining the feasibility of siting a repository for commercial high-level nuclear wastes at Yucca Mountain on and adjacent to the Nevada Test Site. A key part of these investigations is examining the effects of nuclear waste canisters on the host formation. The insertion of such canisters is expected to perturb the naturally occurring hydrology in various ways due in large part to the heat generation of the decaying radionuclides. In order to properly predict long-term migration of nuclides, the basic mechanisms governing water transport through the host rock must be well understood. Although considerable effort has been expended in the study of water transport through soils, the same level of motivation has only recently appeared for studying similar phenomena in rocks such as tuff, granite, sandstone, and shale, which may in some cases be six orders of magnitude lower in permeability than soils. The small pore sizes of these materials (significant pore volume for diameters $< 10^{-8}$ m) lead to capillary-dominated flow for partially saturated conditions.

For rocks of intermediate permeabilities, such as sandstone, previous emphasis has been on relative permeability measurement and capillary pressure curves [1-3]. The present work emphasizes the direct measurement of saturation profiles

obtained in connection with drying phenomena in tight rocks (tuff), since this is pertinent to waste disposal scenarios. This paper extends the author's previous drying experiments [4] with a much better diagnostic technique which allows the measurement of average saturation at a large number of positions along the length of the rock sample.

Saturation measurement using gamma ray densitometry was introduced more than a decade ago in the study of water transport through soils [5,6]. The method depends on the increased attenuation of gamma ray photons when additional water is present in a given region of a porous material. When used to study soils, two different photon energies have been employed since the soil matrix density could change with moisture content. With consolidated rocks such as tuff this is unnecessary and a single photon energy is used. In the present work this technique has been successfully applied to the measurement of saturation profiles in welded tuff, producing a spatial resolution of 3 mm (1/8") and measurements of saturation accurate to ± 8%.

II. EXPERIMENTAL METHOD

Saturation of the welded tuff samples reported herein was determined by measuring the change in attenuation of a beam of 662 keV gamma rays as the samples' water content changed. The beam attenuation was compared with two reference states (totally dry, fully saturated) in order to compute the saturation. The beam was collimated to a diameter of 0.0032 m (1/8") and the sample moved through the beam in order to provide adequate spatial resolution.

Gamma ray photons are scattered from their incident direction primarily through interactions with the electrons in the scattering medium. As a result, attenuation of the beam is expressed by the familiar exponential formula

$$I = I_o \, e^{-\sum_{i=1}^{n} \rho_i \gamma_i z_i} \qquad (1)$$

where I_o is the incident intensity, I the attenuated intensity, ρ_i, γ_i, z_i the density, absorption coefficient, and thickness, respectively of the i^{th} material. Note that γ_i is an atomic constant that does not depend upon the physical form of the substance, but only upon its atomic constituency. Thus γ is the same for pure water, steam or ice.

If one separates attenuation due to water from that due to all other sources, equation (1) may be conveniently rewritten

$$I = I_{dry}\, e^{-\rho_{H_2O}\, \gamma_{H_2O}\, z_{H_2O}} \tag{2}$$

where I_{dry} is the measured intensity with the sample dry. If we assume on the average

$$z_{H_2O} = \phi\ s\ \ell \tag{3}$$

where ϕ is the average porosity across the beam line of sight, s is the saturation, and ℓ the beam path length through the sample, then (2) may be written

$$I = I_{dry}\, e^{-\rho_{H_2O}\, \gamma_{H_2O}\, \phi\ s\ \ell} \tag{4}$$

At a given spatial location and beam orientation, two measurements of I in which the sample is first fully saturated and then totally dried produce ϕ through the relation

$$\phi = -\frac{1}{\rho_{H_2O}\, \gamma_{H_2O}\, \ell} \ln \frac{I_{wet}}{I_{dry}} \tag{5}$$

provided other materials in the beam path remain unchanged between measurements. Once such measurements have been made at each location of interest, the line average saturation at that location is obtained from a new measurement of I by

$$s = \frac{\ell n \frac{I}{I_{dry}}}{\ell n \frac{I_{wet}}{I_{dry}}} \qquad (6)$$

In practice, the beam intensity I is measured by first converting the gamma ray photons to visible photons and then detecting the latter by a conventional photomultiplier tube. At high intensities, the conversion efficiency may depend on the intensity due to pile-up of pulses in the counting electronics components. As a result, the relationship between the count rate R read from the counter and the intensity of incident photons will be nonlinear. This relationship has been found to be of the form

$$R = \frac{I}{1 + \tau I} \qquad (7)$$

where the parameter τ has dimensions of time and corresponds to the response time of the detector/electronics package [7]. Since τ is easily measured, this complication presents no serious difficulty in the use of equation (6), as a rearrangement of (7) allows one to convert count rates to intensities. For the present experiment τ was measured using a variable attenuation technique [8] and found to vary with R according to

$$\tau(R) = 2.5 \times 10^{-6} + 10^{-16} R^2 \quad \text{(sec)} \qquad (8)$$

where R is expressed in counts/sec.

In order to utilize the method just described, the sample is "indexed" at each desired location prior to the moisture migration experiment by taking count rate data both wet and dry. It is thus essential that provision be made for relocating the sample precisely at a given position after saturation, drying or any other interim procedure. It is also essential that none of the other materials in the beam path (e.g. thermal insulation, heater tape) move during the time between initial indexing and final data. Failure to meet either of these conditions could generate unpredictable error in the data.

An estimate of the expected error in the saturation may be derived in a straightforward manner [8] from equations (4)-(7) plus the statistical relation

$$\frac{dN}{N} = \frac{1}{\sqrt{N}} \tag{9}$$

where N is the number of counts obtained during a single measurement. Equation (9) reflects the statistical uncertainty of one standard deviation for a Gaussian distribution. The result for the uncertainty in saturation is

$$|\Delta s| = \left[\sqrt{Rt}\ (1 - \tau R)\ \ell n\ \frac{I_{dry}}{I_{wet}}\right]^{-1} \tag{10}$$

where t is the count time for a single measurement, and R is the associated count rate. Note that the error is proportional to $N^{-1/2}$ so that reasonable increases in count

time only give modest improvements in accuracy. For the present experiments, we had $R \sim 40000\ s^{-1}$, $t = 30$ s, $I_{dry}/I_{wet} = 1.06$ to give $|\Delta s| = .017$. The actual error in s is believed to be more like $\pm$ .08 due to statistical error beyond the one standard deviation region in addition to other sources of error. The latter category includes temperature drift of the detector/electronics package and positioning error of the translation stage.

III. DESCRIPTION OF APPARATUS

A schematic of the apparatus is shown in fig. 1. The sample chamber was attached to a Summit 6106 single axis precision translation table located between the gamma source and detector vaults. The two lead vaults and the translation stage were mounted securely to a steel bench to maintain alignment. The translation table could be positioned either horizontally or vertically and provided a positional resolution of ± 25 μm (0.008 beam diameters).

For the drying experiments, dry N_2 was passed through a valve and flow gauge to a flexible coil of copper tubing wrapped with heater tape. This arrangement allowed gas inlet temperatures as high as 180°C. Gas exiting the chamber was passed through four removable desiccant cartridges [4] arranged in series in order to provide a measurement of water loss rate during the experiments. For the imbibition experiment, the translation table was positioned vertically with all flow tubes disconnected.

Gamma rays were produced by a 5 Curie cesium 137 source contained in a lead vault and collimated to 3 mm (1/8") diameter by a 0.075 m long lead cylinder followed by a 0.15 m long stainless steel cylinder. Photons passing unscattered through the sample chamber were further attenuated with a 0.02 m thick steel block before entering the detector. This was done in order to keep the count rate well below the maximum rate the detector could process (~ 100,000 c/s).

Operation near this regime later was found to give unpredictable results due to detector saturation and/or pulse pileup.

The detector/preamp and counting electronics modules were all standard commercially available units made by Canberra, Inc. The following is a list of major components:

802-4	NaI detector
2007P	preamp
2020	spectroscopy amp
2030	single channel analyzer
2050	gain stabilizer
1776	counter/timer
1788	computer interface

Both experiment control and data analysis were accomplished with a Cromenco System III microcomputer with flexible disc storage. A single master program moved the translation stage to predetermined locations, initiated and terminated the counter/timer and computed count rates. Position and count rate data was then printed in an Integral Data Systems 440 line printer and stored on disc. Upon experiment termination, saturation vs position was computed using a separate program, and plotted on a Hewlett Packard 7225A plotter. During this computation, intensities were determined from equation (7) using count rates corrected for system drift The latter was determined by regularly taking data off the end of the sample where no change in attenuation was

expected. Ratios of these count rates were then used as correction factors for count rates taken through the sample.

A more detailed view of the sample chamber is shown in fig. 2. The chamber outer wall was 6.35 mm (0.25") thick Aℓ with O-ring sealed end caps. The actual sample holder was 3.17 mm (0.125") thick Aℓ and was welded to one of the end caps. The holder held the tuff core firmly in place with set screws and had viewing windows milled out 180° apart in order to present minimum attenuation, a feature that turned out to be unnecessary. This sample holder design proved convenient since samples could be removed from the bench (but kept in the holder) for saturation or drying in an oven and replaced without altering their position relative to the gamma beam. Two fittings in one end cap accepted sheathed thermocouples for measurement of sample temperature at each end. Fittings in the other end cap allowed N_2 gas in and out. Heater tape was wound around the exterior chamber wall and secured by ring clamps to keep it from moving. Fiberglass insulation was wrapped around the entire chamber during drying experiments and taped in place.

For the imbibition experiment, the sample chamber was mounted vertically, with one end cap left off to allow air to escape from the sample. Here water was poured in from the top using a funnel to a level that was maintained just below the top of the sample. The water level was important only to keep the gamma beam water path length outside the sample constant.

IV. SAMPLE PREPARATION AND EXPERIMENTAL PROCEDURE

This work reports water migration results for a single geological material, welded tuff, as this particular volcanic rock is under consideration as a host material for the storage of radioactive waste canisters. The sample used in this study was obtained from the welded Grouse Canyon Member of the Belted Range tuffs located in Southwestern Nevada. The sample was a machined cylindrical core 0.0475 m in diameter, free of obvious fractures, and 0.153 m in length.

The sample was coated with epoxy in order to keep the results as one-dimensional as possible. TRA-CAST BC-3103 epoxy was applied on all surfaces but one end face of the core prior to saturation. When fully cured, this epoxy withstood the high temperatures (~ 185°C) and provided an apparently vapor-tight seal around the circumference of the sample. This conclusion was strengthened by the observation that the epoxy bond was stronger than the rock itself, causing rock fractures to occur when the epoxy was later chipped off.

Considerable effort was then expended to insure that the sample was fully saturated with water before the drying experiment commenced. Typical saturation methods in use today range from simply immersing a specimen in a container of water (hereafter referred to as the "container method") to more sophisticated techniques involving vacuum

pumps and high pressure chambers. Very little information concerning saturation techniques appears in print. The only reference the author could find was that of Brace [9] whose method is utilized by others [10]. In this method, rocks to be saturated were suspended above a container of water in a vacuum for a few hours, dropped into the water, after which the container and sample were subjected to high pressures for a period of "a day or so". Brace's work still leaves several questions unanswered for rocks other than those investigated by him:

1) How long does it take to pump the air out of a sample of given composition and size?
2) How long does it take to completely imbibe water into a sample of given composition and size.
3) Is the pressurization step necessary?
4) How much improvement do complicated techniques offer over the "container method"?

The following is a description of the procedure used for the experiments reported here together with some ancillary experiments designed to at least partially answer the above questions.

The saturation apparatus used here is shown schematically in fig. 3. The sample is dried in an oven and then placed in the bell jar. A vacuum is pulled on the bell jar with valve B open and valves A and C closed. At periodic intervals a check is made to see if the sample is finished

de-gassing by closing valve B and monitoring the rate of pressure rise from the transducer output. This may be compared with the "leak rate" of the system measured with no sample in the jar. The pressure rise rate with the sample in place will approach the latter only when the air pressure inside the sample has equilibrated with that of the bell jar (in this case ~ 4 mm Hg). The maximum deviation from 100% saturation due to the presence of trapped air may be estimated at this point by reducing the remaining volume of air in the sample to its value at one atmosphere and comparing this volume to the total available pore volume. For the present case, this estimate gave values of saturation no lower than 99.5%. Although this was adequate for the present suite of experiments, one could clearly do better by making improvements in the vacuum system. In any case, the pressure rise rate measurement affords one concrete knowledge of whether or not the sample has finished de-gassing.

For the next step, valve B is closed and valve A is opened under water so as to quickly flood the bell jar with water. Although some air will come out of solution in the water during this process, it should not have time to penetrate into the rock. [If it is concluded that this is indeed a problem, it could be remedied by putting the container of water at A in a separate closed container and pumping down to rid the water of dissolved gases. Here the pressure could be restored to atmospheric just prior to flooding the

bell jar.] As the water level nears the top of the bell jar, a vacuum line is connected to valve D, and valves C and D opened to pull water into the manometer tube to a reasonable level as shown. Once this is accomplished, valve A is closed and D is opened to the atmosphere. At this point, any imbibition of water into the sample will be directly reflected in the height of the manometer meniscus. Since this is only true when the water temperature in the bell jar is constant, heater tape and a temperature controller must be added to keep the water temperature elevated slightly above the highest expected room temperature. If the water at A is preheated, prior to flooding the bell jar, at the same temperature that the temperature controller is set for, then the meniscus position provides a direct real time measurement of the water imbibed into the sample. Whenever the meniscus position drops near the bottom of the tube, a vacuum is pulled at D as before and valve A opened slightly to restore the meniscus position.

Data taken during the saturation of the epoxy-covered tuff sample used for the experiments reported here are shown in fig. 4. As can be seen, the saturation time for this sample was about two weeks, with some scatter in the meniscus position being due to extreme room temperature variations. The product of total sample volume (272.8 mℓ) and average porosity determined from the gamma beam (0.144) is 39.3 mℓ, in good agreement with the measured volume of

water imbibed. In general, saturation time will depend on rock permeability and capillary pressure. Since permeability is not usually known to any degree of accuracy, saturation time must be determined experimentally in order to insure complete saturation.

The first two questions raised earlier have now been satisfactorily answered with regard to the present method since the time necessary for de-gassing and resaturation may be measured. The fourth question has been addressed (at least for welded tuff) by saturating two different 0.2 Kgm samples by both the container method and the bell jar apparatus and comparing weight gain. One sample was coated with epoxy in a manner similar to the larger core described previously, the other left uncoated. In both cases, the mass gain while being saturated in an open container continued to increase slightly (even after 15 days for the coated sample), but never exceeded 86% of that obtained by the bell jar technique. It would thus appear that, at least for low permeability materials such as welded tuff, better than 14% of the pores remain air-filled unless some attempt is made to remove the air prior to saturation.

At this point, question 3 remains unanswered in a definitive sense. To the author's knowledge, no attempt has ever been made to quantitatively assess the value of applying high pressures to a sample which has been previously evacuated and then backfilled with water. One might speculate

that air-filled pores would reappear after depressurization due to gas coming back out of solution. However, a more solid understanding here must await further experimental studies.

After resaturation, samples were inserted into the drying chamber, and a reference scan was made. The drying experiments were initiated by starting the flow of N_2 gas and turning on one or both heaters. Although an attempt was made to measure the mass loss rate of water by means of a system of dessicant canisters [4], this was abandoned due to water condensation in the gas flow lines whenever the flow was interrupted. Short interruptions were necessary on occasion to change gas bottles. Several additional scans were taken with the gamma beam at irregular intervals during the experiments. All scans were controlled by a Cromemco microcomputer so that the same beam positions were repeated for each scan. The experiment was continued until count rates at positions throughout the sample indicated no further water loss was occurring. Using information from the first and last scans, saturation as a function of position for any intermediate scan was determined from equations given earlier.

The procedure for the imbibition experiment was different only in that the sample was inserted into the chamber after having been dried during the TUFF 9 drying experiment. After the imbibition experiment was terminated, the sample was then redried in an oven and resaturated before taking the final (wet) scan.

V. EXPERIMENTAL RESULTS

Some information concerning the variations in pore distribution in the tuff sample may be obtained by combining porosity measurements from the three drying experiments. Inhomogeneity is present both axially and rotationally, the latter being due to azimuthal variations which show up as a difference between experiments since no special care was taken to keep from rotating the samples prior to commencing a new experiment. Results for sample porosity as a function of axial position are shown in fig. 5. Here it is apparent that, at least for the orientations used, the front two-thirds of the sample is relatively homogeneous for rays passing through the axis. Near the rear of the sample, however, considerably lower porosity was measured for the orientation of TUFF 9. Overall uncertainty in the porosity measurement is estimated to be ± .01.

Results from the three drying experiments and the imbibition experiment are shown in figs. 6-9 as plots of saturation vs. axial position for different scans. Since each scan took from 10-20 minutes, the curves are not exactly "snapshots" of saturation profiles. However, in most cases, changes of saturation occurred on a time scale of hours, so that the error incurred by viewing the curves as having been produced instantaneously should not be too great. The time and temperature appropriate for the start of each scan is shown next to the curve. For the drying experiments, the position where the curves commence between 0.01 and 0.02 meters

corresponds to the drying surface across which N_2 was passed. For the imbibition experiment, the same position is the surface through which water was imbibed (the bottom surface). Overall uncertainty in the saturation is estimated to be ± 8%. This figure is the combined result of electronics drift, statistical error, and error from the positioning table. The latter variable is of particular importance near areas of high count rate gradient.

Results from the first drying experiment (TUFF 7, fig. 6) show unmistakebly that even for a low permeability material such as welded tuff ($k = 10^{-15}$-10^{-18} m^2) drying takes place simultaneously throughout the length of the sample. This occurs in the other experiments also, and is in sharp disagreement with previous "evaporation front" models used to describe the drying of tuff [4]. More striking, however, is the hump in the saturation curve near the drying surface at late time. For this experiment, the sample actually dried faster near the epoxy-covered end than near the drying surface. This probably occurred as a result of cooling of the drying end by the N_2 gas stream, and subsequent migration of H_2O in both phases toward that end under the action of the corresponding vapor-pressure gradients.

In order to test the above hypothesis, a heater was added to the gas stream in order to provide control of the axial temperature. The second experiment (TUFF 8, fig. 7) was performed with heaters adjusted to give nearly isothermal

conditions. In the resulting profiles, the hump noticed previously at late time is gone. It appears that a sample dried isothermally is characterized by a plateau of nearly constant saturation which decreases with time. (This holds everywhere except very near the drying surface where a region of steep gradient matches the plateau to the S = 0 boundary condition.) This suggests that isothermal drying might provide a convenient means of producing uniformly saturated samples of a given partial saturation. Here it is assumed that, once the drying was terminated, the steep gradient region near the drying surface would disappear rather quickly due to capillary forces.

The third drying experiment was performed using only the heated gas stream to heat the sample. This experiment (TUFF 9, fig. 8) thus provided a temperature gradient of about 230 K/m in the direction of water migration. The results are strikingly different from the TUFF 7 experiment in that the region near the drying surface dried out completely, leaving all the liquid water in the other end. This is consistent with the vapor pressure gradient opposing the motion of liquid water. Also, the early time data has the distinct appearance of a receding evaporation front, except that the plateau behind the front does not stay at 100%, but rather decreases with time in a manner similar to that of the isothermal experiment. Although this result does not substantiate the validity of the evaporation front

model as an accurate description of the moisture transport, it does seem to indicate that for certain boundary conditions, evaporation front models may give reasonable results. This is consistent with previous calculations made of water loss rates for an in-situ heater experiment at the Nevada Test Site [11]. In this case the temperature gradient was in the same direction relative to the direction of moisture movement as in TUFF 9, and results obtained using an evaporation front model gave reasonably good agreement with experiment. It is now felt that this result was not fortuitous but rather is consistent at least in part with the results reported here.

Lastly, an imbibition experiment (TUFF 10) was performed in order to quantify the effects of capillary forces on water transport. The results from this experiment are shown in fig. 9. First of all, it is apparent from both the drying and imbibition results that the saturation profiles do not in general display a front-like character. Rather, the results more closely resemble what one would expect from the solution to a diffusion equation. For example, we see that at t = 4 hrs some water has found its way to the other end of the sample even though the saturation in most areas is still below 25%. Later on, at t = 1 day, the profile shows an oscillatory appearance. At present, the reason for this curve shape is unknown, and in fact it would appear difficult to predict such a shape from any one model. It is

possible that the sample has some inhomogeneity which was not detected in the porosity measurements. After a period of 6 days, the experiment was terminated, though the sample was still not fully saturated. This is consistent with the saturation testing described in section IV. It was found there that samples simply immersed in water only saturated to a level of about 85% due to trapped air. This figure agrees quite well with TUFF 10 data at all but the upper end (> 0.12 m) where apparently the saturation was still rising.

VI. CONCLUSION

This set of experiments has demonstrated clearly the usefulness of gamma beam densitometry as a saturation diagnostic for water transport through porous rock. The method has been shown to be fairly accurate, possess good spatial resolution and to be totally unobtrusive. The system is relatively inexpensive and easy to operate.

One-dimensional water transport experiments have been conducted on a 0.15 m long core of welded tuff. Pre-saturation of the sample for the drying experiments was accomplished using a bell jar evacuation technique, which was shown to give superior results compared with simple immersion methods. Results of the drying experiments show that the shapes of the saturation profiles depend on the presence and direction of the sample temperature gradient. Profiles from all three drying experiments show that drying takes place simultaneously throughout the sample, and not from an isolated region such as an evaporation front. However, profiles for the case of a temperature gradient aligned with the direction of moisture transport do resemble to some degree evaporation front profiles.

Results from the imbibition experiment show capillary forces to be important for welded tuff. This conclusion follows from the fact that water filled the full length of the sample to a saturation level of 20% in a matter of 4 hrs. This flow rate is not much less than those obtained while

drying the rock at temperatures above 180°C. This result implies that drying theories to be used to model tight rock formations such as welded tuff should take into account capillary effects.

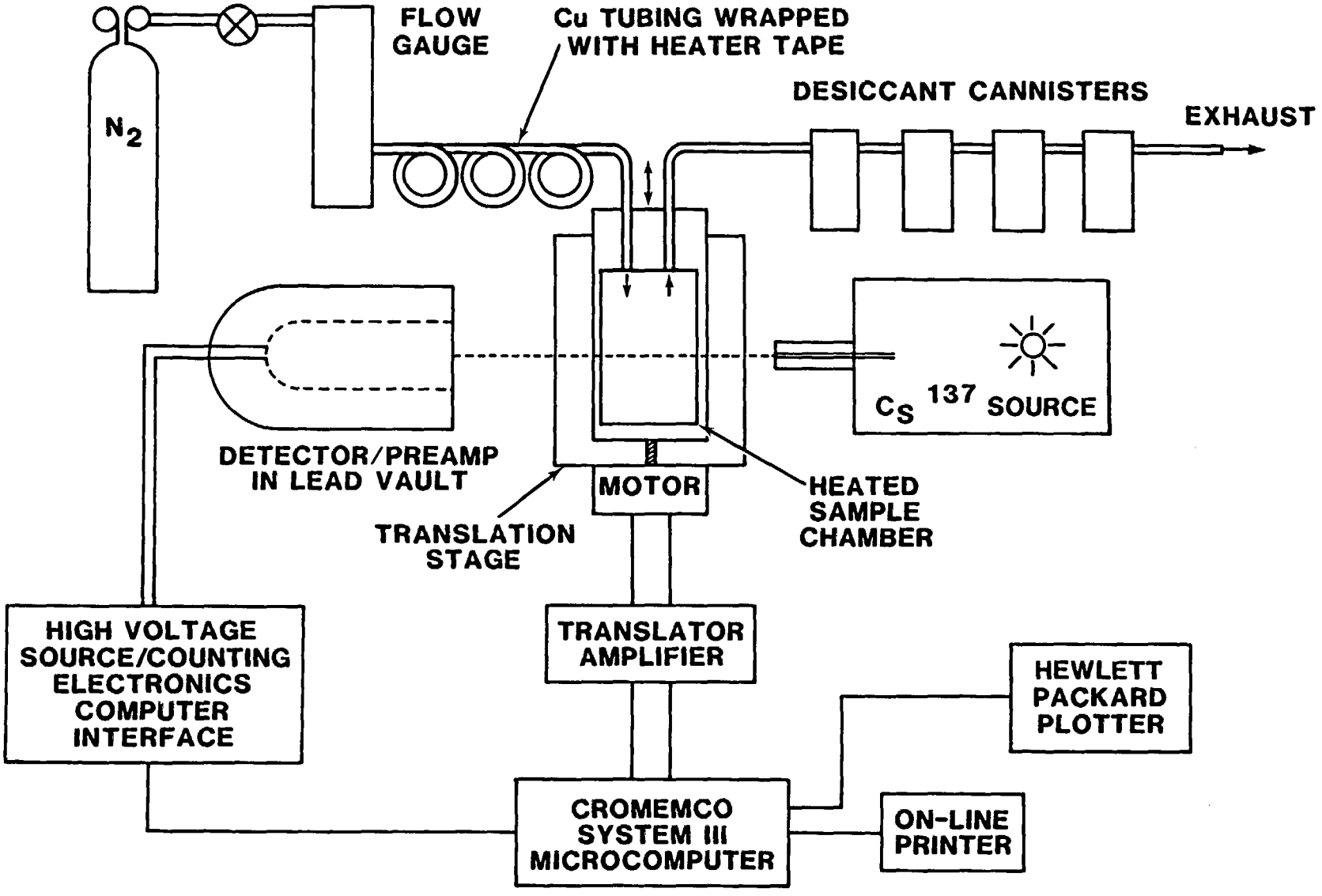

Figure 1. Schematic diagram of experimental apparatus

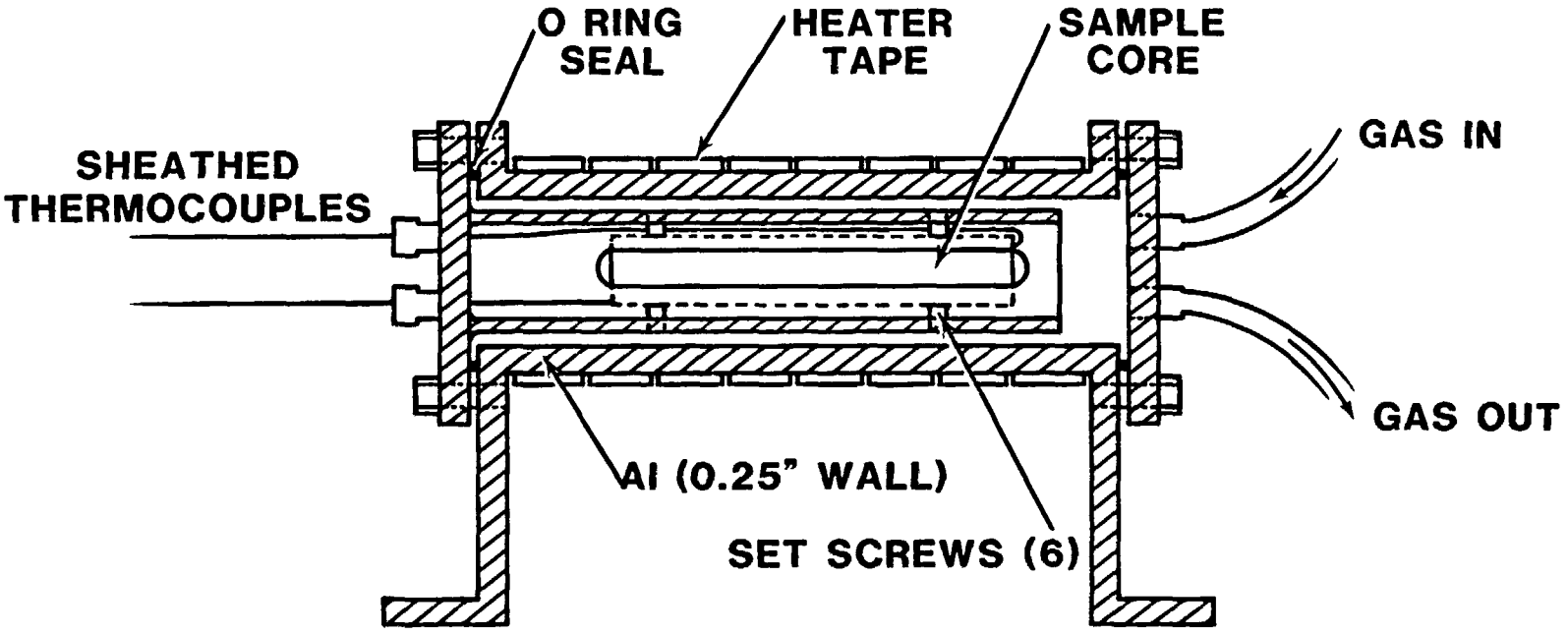

Figure 2. Sectional view of sample chamber

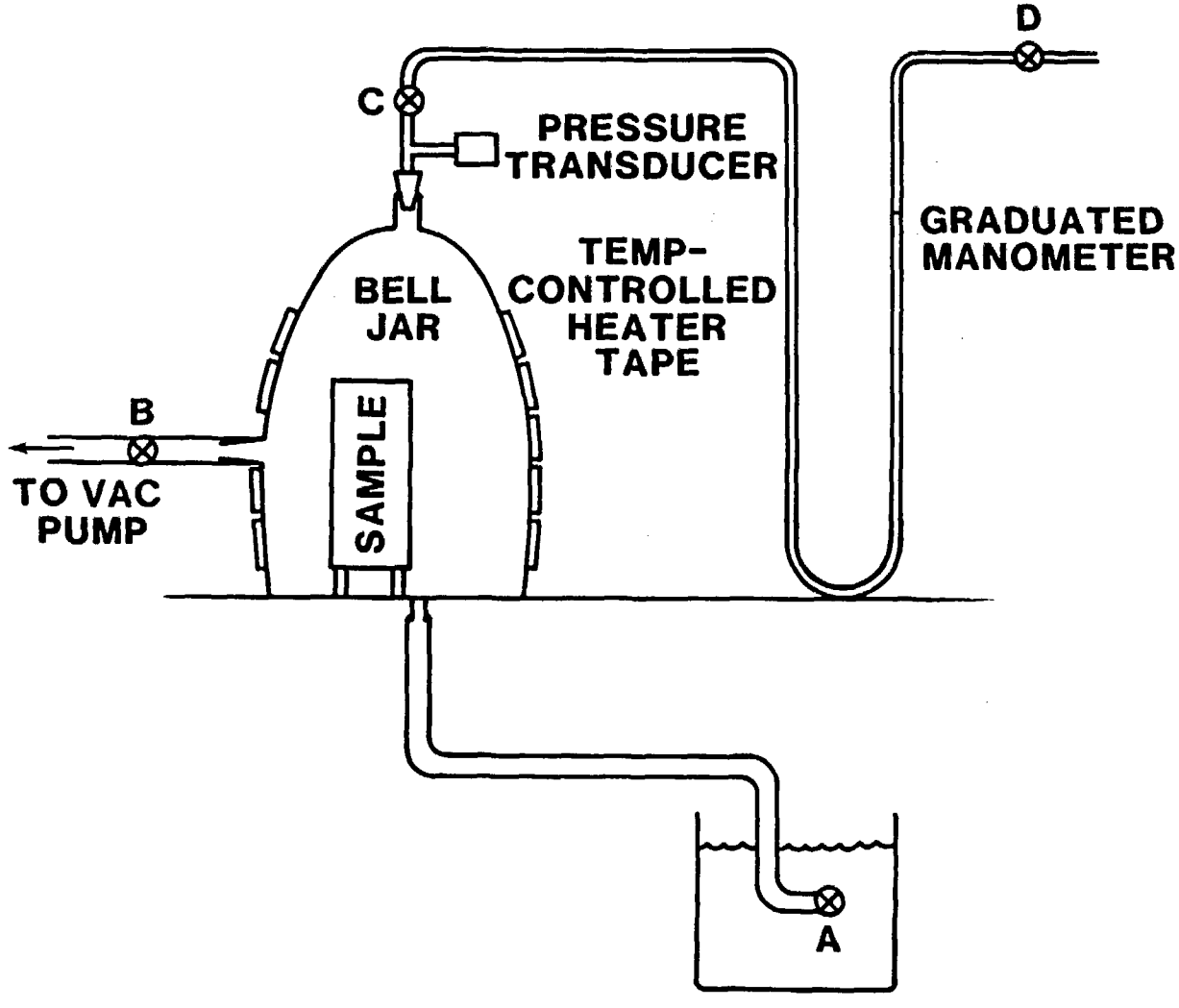

Figure 3. Saturation apparatus

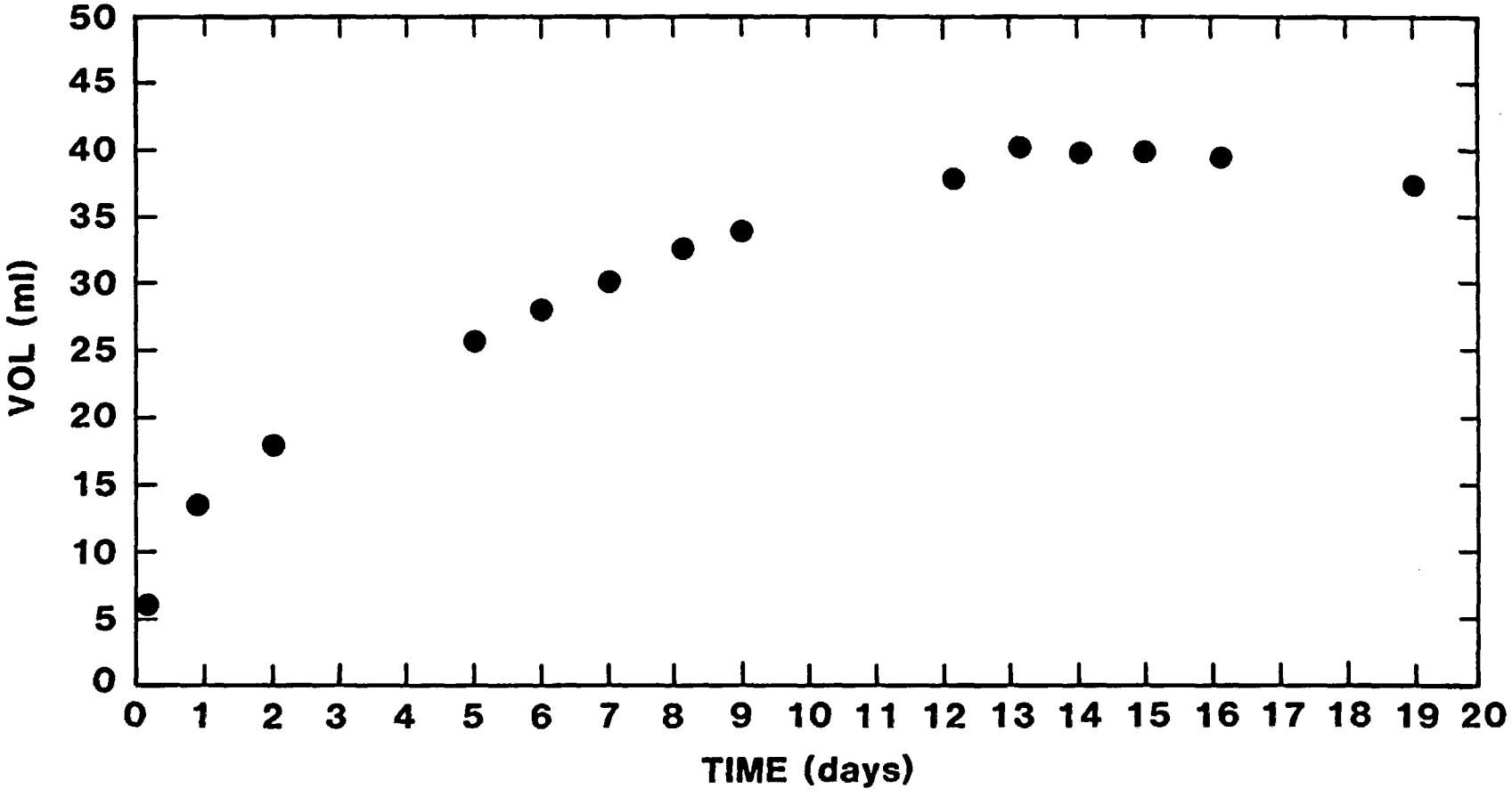

Figure 4. Imbibed volume vs. time during saturation for sample used in drying-imbibition experiments

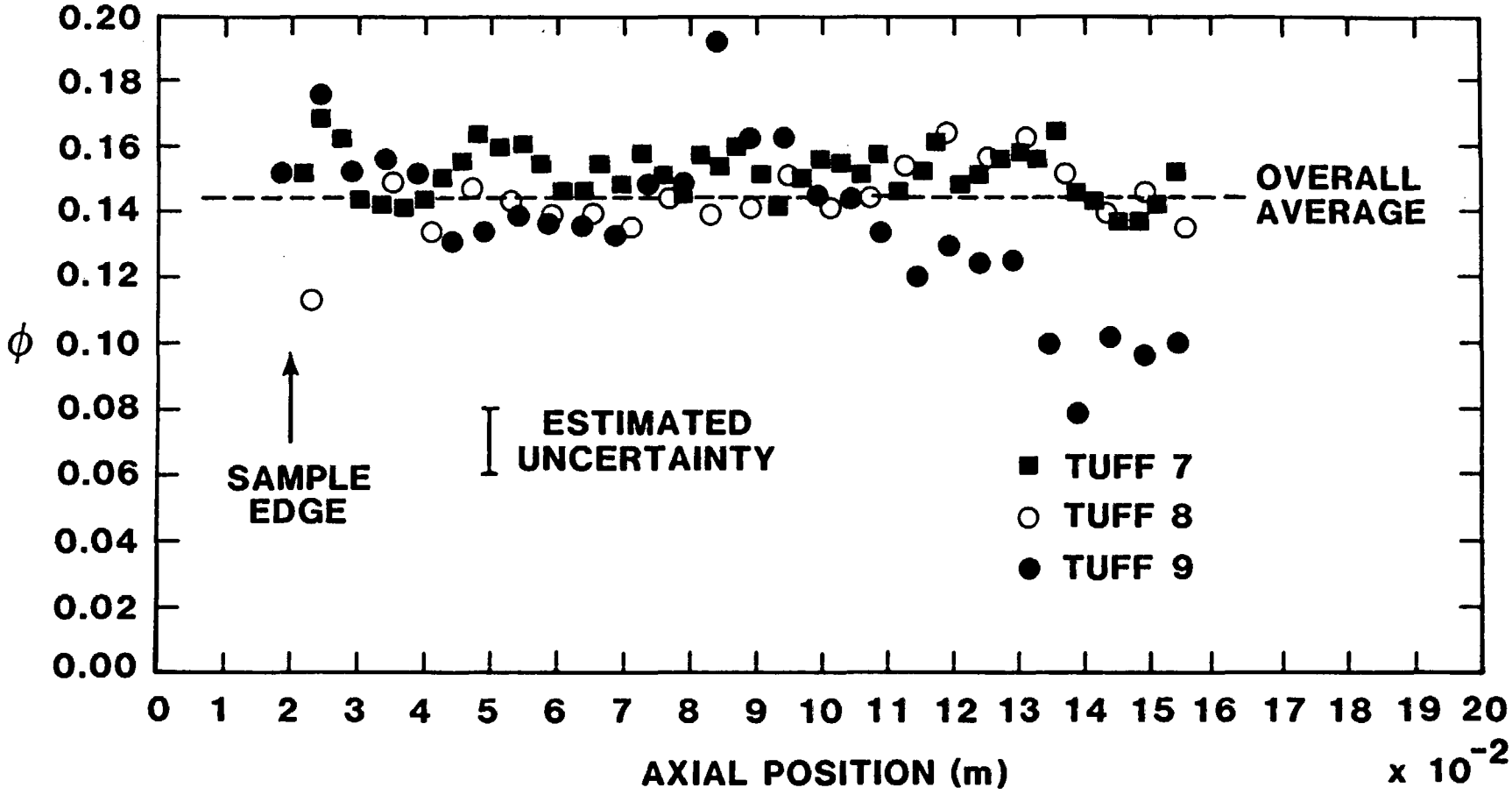

Figure 5. Porosity vs. axial position for tuff sample

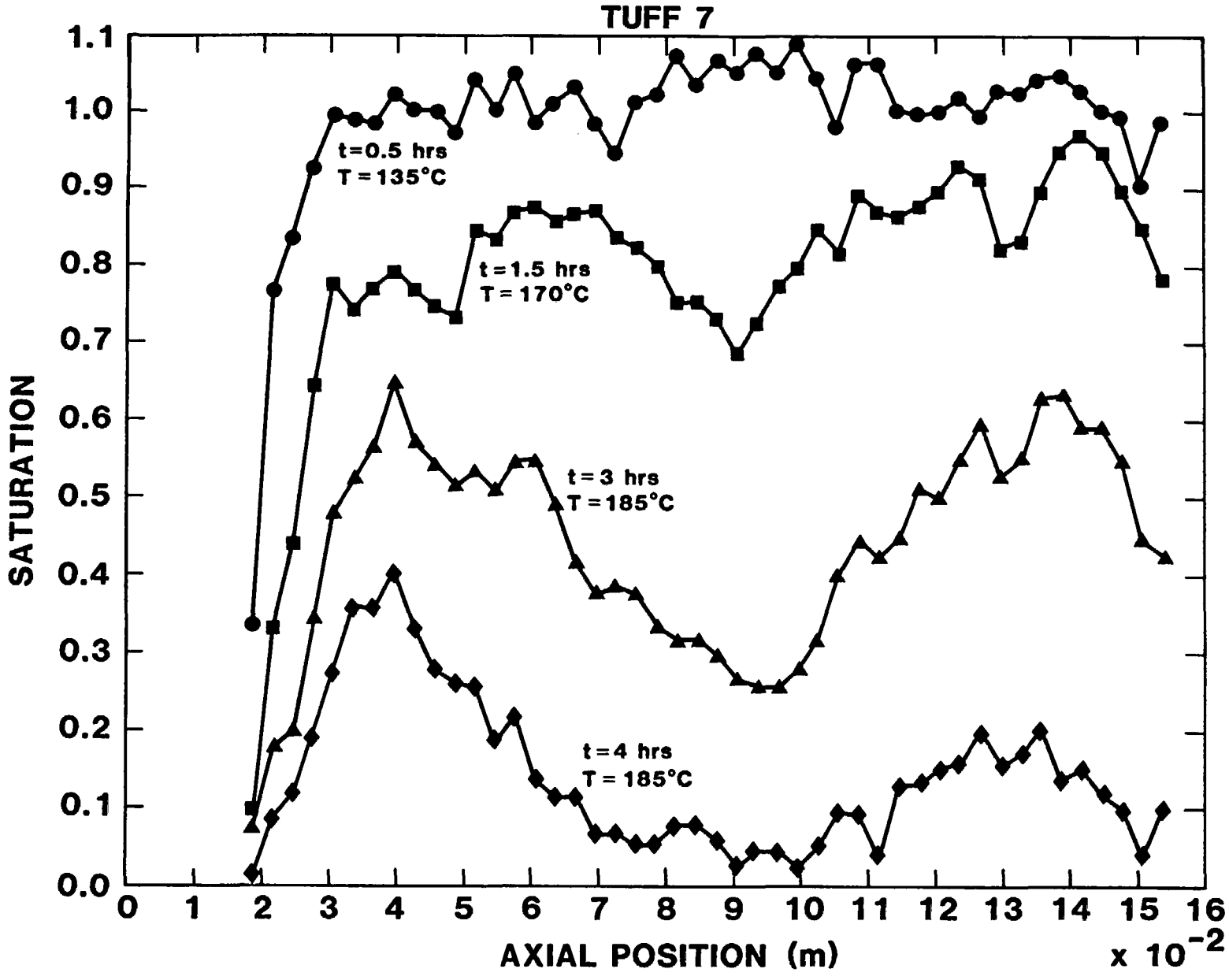

Figure 6. Saturation profiles for the Tuff 7 experiment

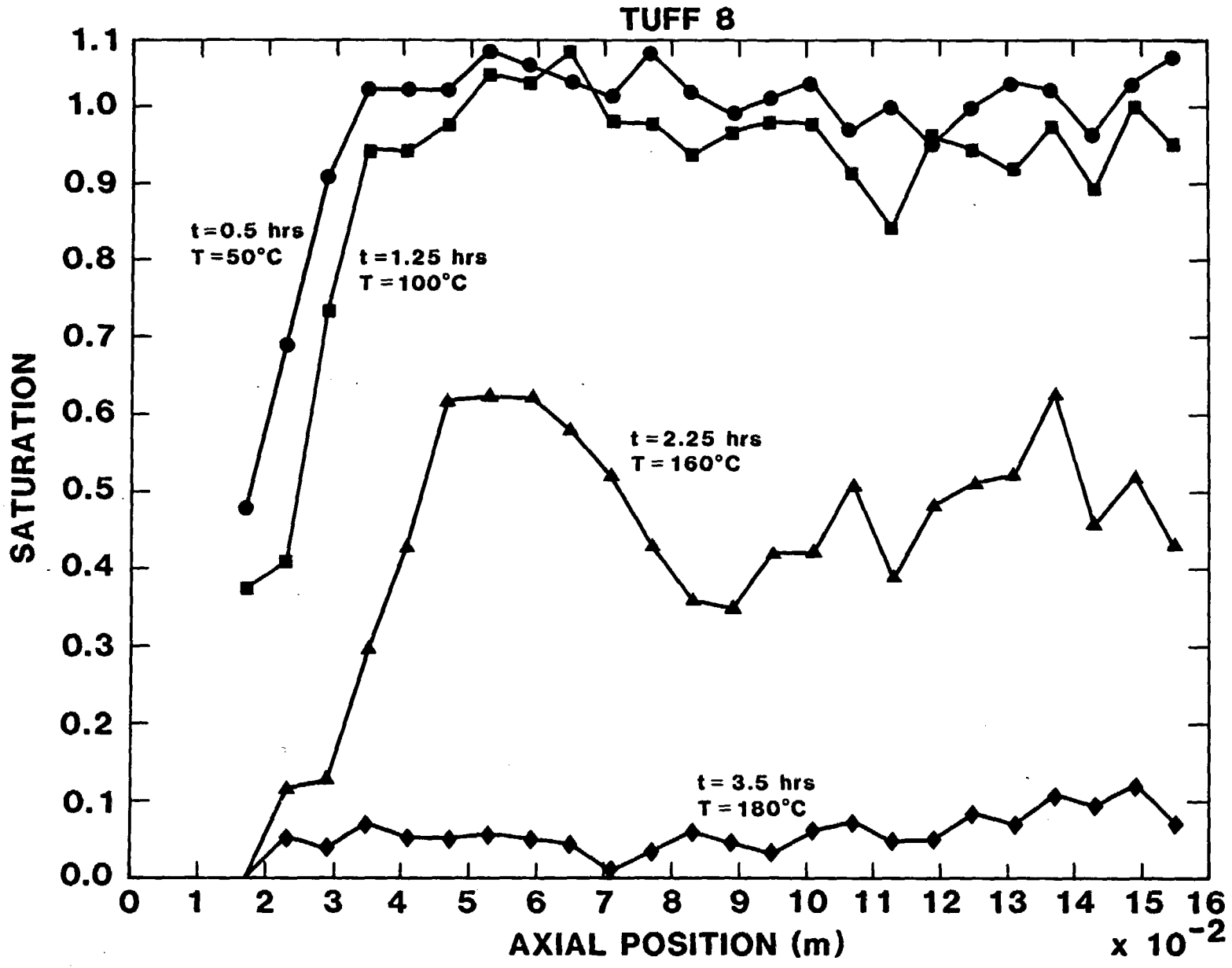

Figure 7. Saturation profiles for the Tuff 8 experiments

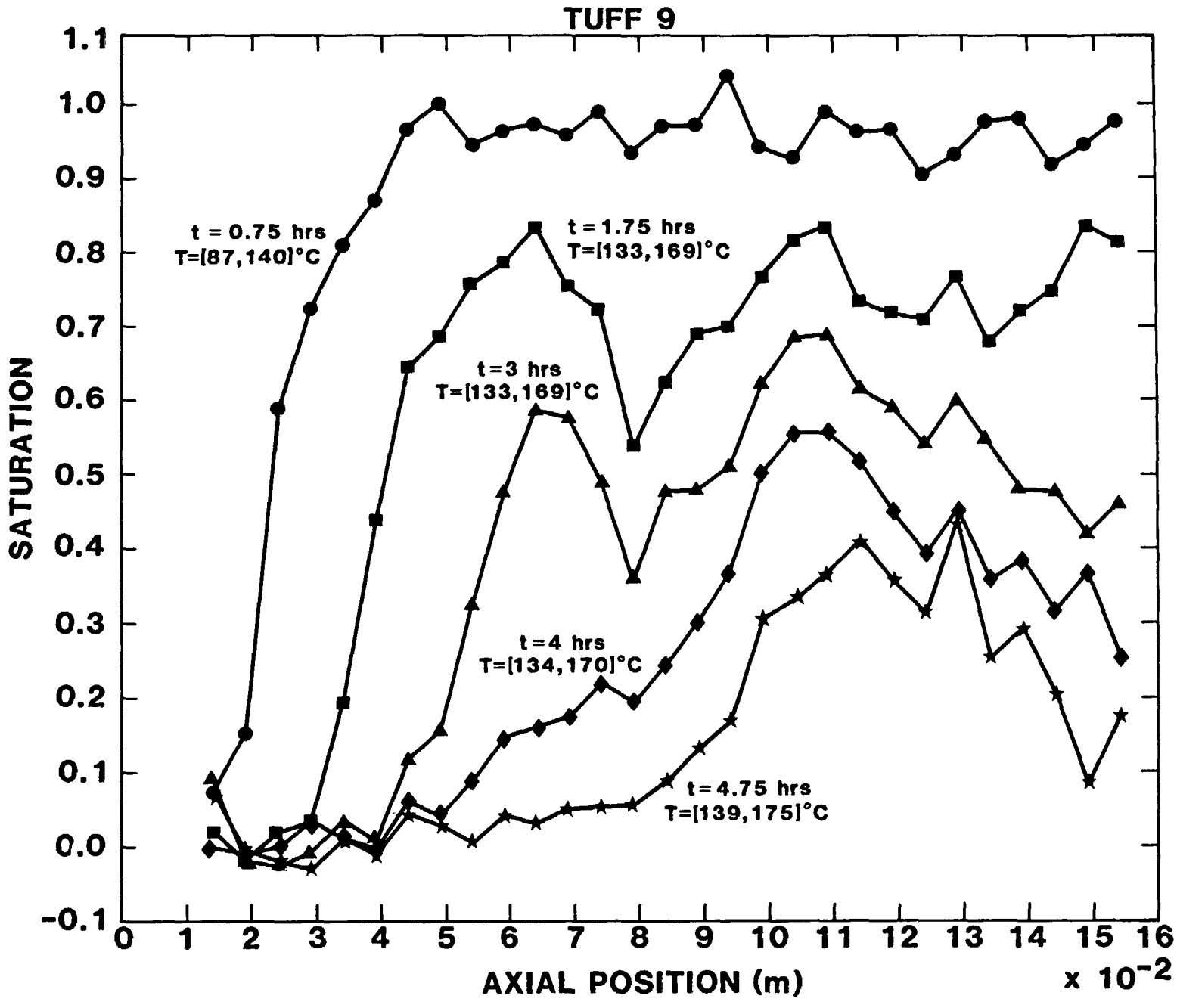

Figure 8. Saturation profiles for the Tuff 9 experiments

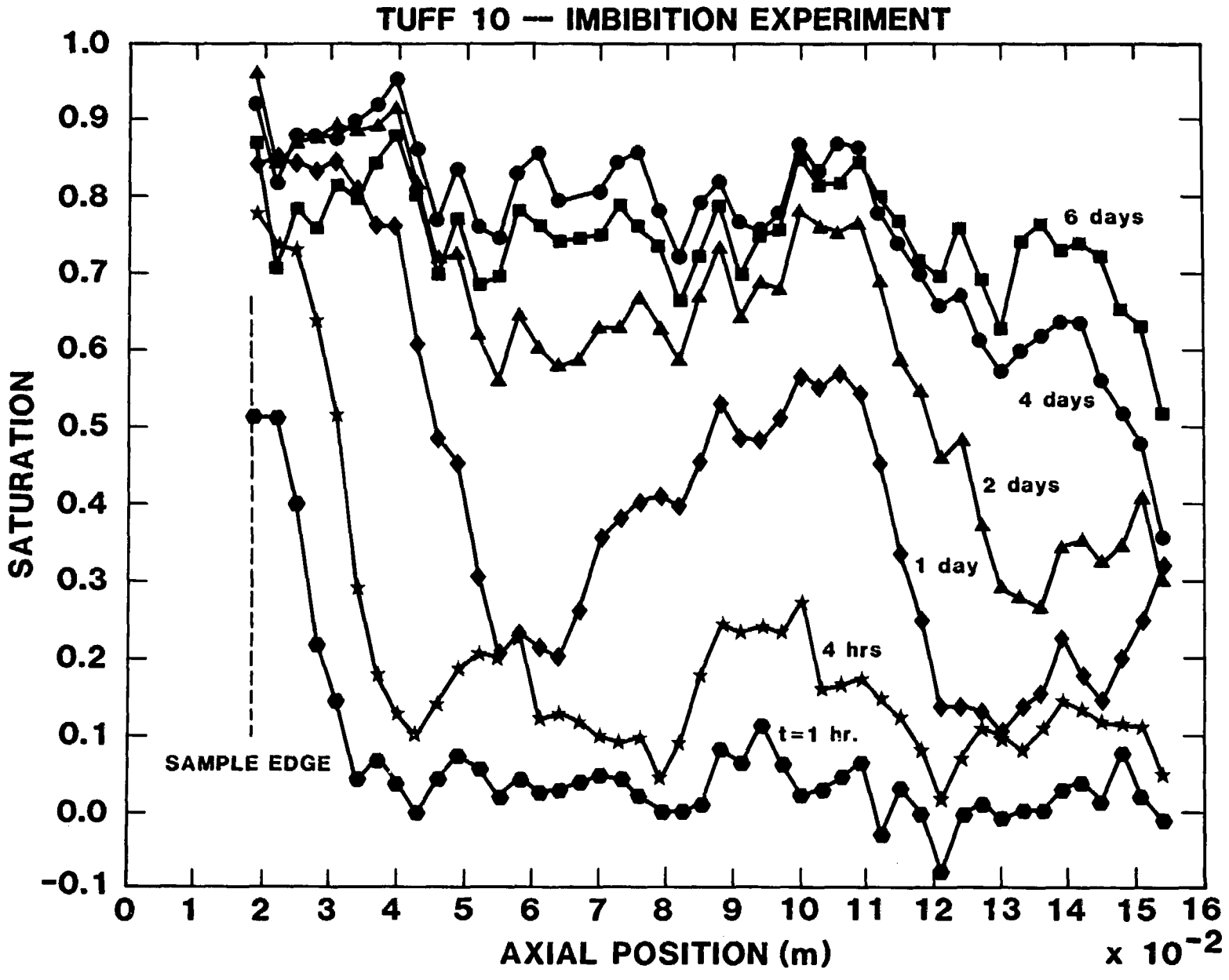

Figure 9. Saturation profiles for the Tuff 10 imbibition experiment

REFERENCES

1. R. H. Brooks and A. T. Corey, "Properties of Porous Media Affecting Fluid Flow", Proc. of ASCE, Vol. 92, No. IR2, p. 61-88 (June, 1966).

2. R. M. Weinbrandt, H. J. Ramey, Jr., F. J. Casse´, "The Effect of Temperature on Relative and Absolute Permeability of Sandstones", Soc. Pet. Eng. Journal, Oct. 1975, p. 376-384.

3. A. T. Corey, C. H. Rathjens, J. H. Henderson, M. R. J. Wyllie, "Three-Phase Relative Permeability", Petroleum trans, AIME, Vol. 207, pp. 349-351 (1956).

4. G. R. Hadley, "Evaporative Water Loss From Welded Tuff", paper presented at Winter Annual Meeting of the ASME, Chicago, Nov. 16-21, 1980, see HTD-Vol. 11, pp. 19-25.

5. W. H. Gardner, G. S. Campbell, C. Calissendorff, "Systematic and Random Errors in Dual Gamma Energy Soil Bulk Density and Water Content Measurements", Proc. Soil Sci. Soc. Amer. 36 (3), pp. 393-398 (1972).

6. W. N. Herkelrath, E. E. Miller, "High Performance Gamma System for Soil Columns", Soil Sci. Soc. Am. Journal, Vol. 40, No. 2, pp. 331-332 (1976).

7. R. D. Evans, Radiation Dosimetry, Vol. 1, pp. 93-155, Academic Press, New York, 1968.

8. D. C. Reda, G. R. Hadley, JE R. Turner, "Application of the Gamma Beam Attenuation Technique to the Measurement of Liquid Saturation for Two-Phase Flows in Porous Media", Proc. of 27th Int'l. Instrumentation Symposium, April 27-30, Indianapolis, pp. 553-568 (1981).

9. W. F. Brace, A. S. Orange, T. R. Madden, "The Effect of Pressure on the Electrical Resistivity of Water-Saturated Crystalline Rocks", JGR Vol. 70, No. 22, pp. 5669-5678 (1965).

10. J. B. Walsh, E. R. Decker, "Effect of Pressure and Saturating Fluid on the Thermal Conductivity of Compact Rock", JGR Vol. 71, No. 12, pp. 3053-3061 (1966).

11. J. K. Johnstone, G. R. Hadley, D. R. Waymire, C. O. Duimstra, "In-Situ Tuff Water Migration-Heater Experiment: Final Report", Sandia National Laboratories Report SAND81-1918 (1981).

J. W. Bennett (RW-20)
Acting Associate Director
Geologic Repository Deployment
U. S. Department of Energy
Washington, DC 20545

Ralph Stein (RW-21)
Acting Deputy Associate Director
Geologic Repository Deployment
U. S. Department of Energy
Washington, DC 20545

J. G. Vlahakis (RW-21)
Geologic Repository Deployment
U. S. Department of Energy
Washington, DC 20545

C. R. Cooley (RW-24)
Acting Director
Geosciences & Technology Division
Geologic Repository Deployment
U. S. Department of Energy
Washington, DC 20545

M. W. Frei (RW-23)
Acting Director
Engineering & Licensing Division
Geologic Repository Deployment
U. S. Department of Energy
Washington, DC 20545

J. J. Fiore (RW-22)
Acting Director
Program Management Division
Geologic Repository Deployment
U. S. Department of Energy
Washington, DC 20545

E. S. Burton (RW-25)
Acting Director
Siting Division
Geologic Repository Deployment
U. S. Department of Energy
Forrestal Building
Washington, DC 20585

S. A. Mann, Manager
Crystalline Rock Project Office
U. S. Department of Energy
9800 S. Cass Avenue
Argonne, IL 60439

T. P. Longo (RW-22)
Geologic Repository Deployment
U. S. Department of Energy
Washington, DC 20545

Cy Klingsberg (RW-24)
Geologic Repository Deployment
U. S. Department of Energy
Washington, DC 20545

J. E. Shaheen (RW-25)
Geologic Repository Deployment
U. S. Department of Energy
Forrestal Building
Washington, DC 20585

Chief, High-Level Waste Technical
Development Branch
Division of Waste Management
U. S. Nuclear Regulatory Commission
Washington, DC 20555

NTS Project Manager
High-Level Waste Technical
Development Branch
Division of Waste Management
U. S. Nuclear Regulatory Commission
Washington, DC 20555

Document Control Center
Division of Waste Management
U. S. Nuclear Regulatory Commission
Washington, DC 20555

J. O. Neff, Program Manager
National Waste Terminal
Storage Program Office
U. S. Department of Energy
505 King Avenue
Columbus, OH 43201

N. E. Carter
Battelle
Office of Nuclear Waste Isolation
505 King Avenue
Columbus, OH 43201

C. H. George (RW-3)
Geologic Repository Deployment
U. S. Department of Energy
Washington, DC 20545

ONWI Library (5)
Battelle
Office of Nuclear Waste Isolation
505 King Avenue
Columbus, OH 43201

O. L. Olson, Project Manager
Basalt Waste Isolation Project Office
U. S. Department of Energy
Richland Operations Office
Post Office Box 550
Richland, WA 99352

E. B. Ash
Rockwell International Atomics
Rockwell Hanford Operations
Richland, WA 99352

A. A. Metry, Program Manager
Roy F. Weston, Inc.
2301 Research Blvd., 3rd Floor
Rockville, MD 20850

G. Tomsic
Utah Dept. of Community
Economic Development
Room 6290, State Office Bldg.
Salt Lake City, UT 89114

P. J. Iverson, Deputy Director
Department of Minerals
State of Nevada
400 West King Street
Carson City, NV 89710

R. R. Loux, Jr.
Department of Minerals
State of Nevada
400 West King Street
Carson City, NV 89710

K. Street, Jr.
Lawrence Livermore National Lab.
Post Office Box 808
Mail Stop L-209
Livermore, CA 94550

W. S. Twenhofel
820 Estes Street
Lakewood, CO 80215

L. D. Ramspott (3)
Technical Project Officer
Lawrence Livermore National Lab.
Post Office Box 808
Mail Stop L-204
Livermore, CA 94550

D. C. Hoffman
Los Alamos National Laboratory
Post Office Box 1663
Mail Stop E-515
Los Alamos, NM 87545

D. T. Oakley (3)
Technical Project Officer
Los Alamos National Laboratory
Post Office Box 1663
Mail Stop F-671
Los Alamos, NM 87545

P. L. Aamodt
Los Alamos National Laboratory
Post Office Box 14100
Las Vegas, NV 89114

R. W. Lynch
Sandia National Laboratory
Post Office Box 5800
Organization 6300
Albuquerque, NM 87185

T. O. Hunter (4)
Technical Project Officer
Sandia National Laboratories
Post Office Box 5800
Organization 6310
Albuquerque, NM 87185

A. R. Hakl, Manager
Westinghouse Electric Corporation
Waste Technology Services Division
Nevada Operations
Post Office Box 708
Mail Stop 703
Mercury, NV 89203

J. A. Cross, Manager
Las Vegas Branch
Fenex & Scisson, Inc.
Post Office Box 15408
Las Vegas, NV 89114

W. W. Dudley, Jr. (3)
Technical Project Officer
U. S. Geological Survey
Post Office Box 25046
Mail Stop 418
Federal Center
Denver, CO 80225

M. E. Spaeth (3)
Technical Project Officer
Science Applications, Inc.
2769 South Highland Drive
Las Vegas, NV 89109

D. L. Vieth, Director (6)
Waste Management Project Office
U. S. Department of Energy
Post Office Box 14100
Las Vegas, NV 89114

D. F. Miller, Director
Office of Public Affairs
U. S. Department of Energy
Post Office Box 14100
Las Vegas, NV 89114

H. D. Cunningham
General Manager
Reynolds Electrical &
Engineering Co., Inc.
Post Office Box 14400
Mail Stop 555
Las Vegas, NV 89114

A. E. Gurrola, General Manager
Energy Support Division
Holmes & Narver, Inc.
P. O. Box 14340
Las Vegas, NV 89114

D. A. Nowack (14)
U. S. Department of Energy
Post Office Box 14100
Las Vegas, NV 89114

B. W. Church, Director
Health Physics Division
U. S. Department of Energy
Post Office Box 14100
Las Vegas, NV 89114

Internal Distribution:

1510 J. W. Nunziato
1511 G. G. Weigand
1511 G. R. Hadley (10)
1511 N. E. Bixler
1511 R. R. Eaton
1511 M. J. Martinez
1512 J. C. Cummings
1512 D. C. Reda
1513 D. W. Larson
1520 D. J. McCloskey
1530 L. W. Davison
1540 W. C. Luth
6310 T. Hunter
6311 L. W. Scully
6312 F. W. Bingham
6312 N. K. Hayden
6312 J. K. Johnstone
6312 R. R. Peters
6312 Y. T. Lin
6313 J. R. Tillerson
6313 J. Fernandez
6313 E. A. Klavetter
6313 B. M. Schwartz
6313 R. M. Zimmerman
6300 R. W. Lynch
6330 W. D. Weart
8024 M. A. Pound
3141 C. M. Ostrander (5)
3151 W. L. Garner (3)
for DOE/TIC (Unlimited Release)
DOE/TIC (28)
(C. H. Dalin, 3154-3)

Org.	Bldg.	Name	Rec'd by	Org.	Bldg.	Name	Rec'd by

Sandia National Laboratories